Composites Part B 130 (2017) 119–131

Contents lists available at ScienceDirect

Composites Part B

journal homepage: www.elsevier.com/locate/compositesb

Development of glass microballoon/HDPE syntactic foams by compression molding

M.L. Jayavardhan [a], B.R. Bharath Kumar [b], Mrityunjay Doddamani [a], Ashish K. Singh [c], Steven E. Zeltmann [c, *], Nikhil Gupta [c]

[a] Advanced Manufacturing Laboratory, Department of Mechanical Engineering, National Institute of Technology Karnataka, Surathkal, India
[b] Department of Mechanical Engineering, Jain College of Engineering and Technology, Hubballi, India
[c] Composite Materials and Mechanics Laboratory, Mechanical and Aerospace Engineering Department, Tandon School of Engineering, New York University, Brooklyn, USA

ARTICLE INFO

Article history:
Received 30 May 2017
Accepted 28 July 2017
Available online 1 August 2017

Keywords:
Syntactic foam
Glass microballoon
High density polyethylene
Mechanical properties

ABSTRACT

Thermoplastic resins are widely used in consumer products and industrial components. There is a significant interest in weight reduction of many of those components. Although glass hollow particle filled lightweight syntactic foams with thermoset matrices have been studied in detail, studies on thermoplastic syntactic foams are scarce. The present study is focused on developing a compression molding based processing method for glass microballoon/high density polyethylene (GMB/HDPE) syntactic foams and studying their mechanical properties to develop structure-property correlations. Blending of GMB in HDPE is carried out using a Brabender mixer with processing parameters optimized for minimal filler breakage. Flexural and tensile test specimens are compression molded with 20, 40 and 60 vol% of GMB. Particle fracture increases with increasing GMB content due to increased particle to particle interaction during processing. Additionally, increasing wall thickness makes GMBs stronger and results in reduced particle fracture. Flexural modulus increases while strength decreases with increasing filler content. Tensile strength decreases with increasing filler content, while tensile modulus is relatively unchanged. GMB volume fraction has a more prominent effect than the wall thickness on the mechanical properties of syntactic foams. Specific moduli of GMB/HDPE foams are superior while specific strength is comparable to neat HDPE.

1. Introduction

Syntactic foams are lightweight composite materials in which hollow particles are embedded in a matrix resin [1,2]. These closed cell foams are widely used in structural applications including buoys, submarine buoyancy modules, underwater vehicle structures, thermoforming plugs, and aircraft components [3]. Thermosetting syntactic foams with epoxy and vinyl ester matrices have been studied for mechanical, thermal and electrical properties in a wide range of published literature [4–10]. Theoretical models and simulations studies are also available on these materials studying parameters such as particle-matrix interfacial effects, debonding, particle failure effects on properties of syntactic foams, and failure modes under complex loading conditions. Initial studies were mostly focused on determining the effect of particle volume fraction on mechanical properties of thermoset matrix syntactic foams [11–13]. However, a combination of GMB wall thickness and volume fraction has resulted in greater control over the properties of syntactic foams [1].

Despite the availability of wide range of literature on thermoset syntactic foams, studies on thermoplastic matrix syntactic foams are relatively scarce. Given the differences in the basic nature of the materials, thermoplastic resins and their composites require different processing methods and the test protocols; therefore, detailed studies on processing and structure-property correlations of thermoplastic matrix syntactic foams are desired. An overview of some of the thermoplastic matrix syntactic foams can be found in chapters of a recent book [14,15].

Injection molding and compression molding are the two widely used processing methods for thermoplastic resins. Injection molding has been used previously for fabricating HDPE matrix

* Corresponding author.
E-mail addresses: mrdoddamani@nitk.edu.in (M. Doddamani), steven.zeltmann@nyu.edu (S.E. Zeltmann), ngupta@nyu.edu (N. Gupta).

http://dx.doi.org/10.1016/j.compositesb.2017.07.037
1359-8368/

Nomenclature

d	Flexural specimen thickness
K	Bulk modulus of syntactic foams
K_m	Bulk modulus of matrix resin
K_i	Bulk modulus of GMB material
r_0	Outer radius of GMBs
L	Flexural specimen span length
E_f	Flexural modulus
η	Radius ratio of GMBs
ρ_t	Theoretical density of syntactic foams
ρ_g	Density of glass
σ_{uf}	Ultimate flexural strength
ε_{uf}	Strain at ultimate flexural stress
σ_{uT}	Ultimate tensile strength
ε_{uT}	Strain at ultimate tensile stress
Φ	Volume fraction of GMBs
m	Slope of the elastic part of the flexural load-deflection curve
G	Shear modulus of syntactic foams
G_m	Shear modulus of matrix resin
G_i	Shear modulus of GMB material
E_f	Flexural modulus
b	Flexural specimen width
E_t	Tensile Modulus
ρ_{TPD}	True particle density of GMBs
ρ_e	Measured density of syntactic foams
w	Wall thickness of GMBs
σ_{ff}	Flexural fracture strength
ε_{ff}	Flexural fracture strain
σ_{fT}	Tensile fracture strength
ε_{fT}	Tensile fracture strain

syntactic foams [16–22], while the present study intends to explore the compression molding process for this purpose. The existing studies used fly ash cenosphere as fillers. Cenospheres possess defects such as surface irregularities, porosity in their walls and non-uniform wall thickness, which compromise their mechanical properties. Syntactic foams intended for load bearing or critical applications tend to use high quality engineered GMBs as fillers due to higher quality and better predictability of properties.

Most of the existing work investigated thermoplastic matrix syntactic foams with up to 30 wt% of particles [23–25], mainly due to the difficulty of fabricating high quality foams with higher particle loading. High particle content can help in lowering the syntactic foam density. The present work deals with reinforcing HDPE with up to 60 vol% of GMBs. Such higher filler loading is expected to help in understanding the limitations of the processing method. GMBs are used in as received condition because coating of particles has shown to increase the clustering effects, change particle size distribution, and the coating thickness variation may introduce another variable in the study [25]. The present work includes initial mixing of GMBs with HDPE using a Brabender mixer followed by compression molding. Flexural and tensile properties are studied for the molded specimens. Generalization of the experimental data is carried out using a theoretical model so that the results of this study can be extended to a wider range of particle wall thicknesses and volume fractions.

2. Experimental methods

2.1. Materials

HDPE (180M50 grade, 20 g/10 min melt flow index), procured from Indian Oil Corporation Ltd., Mumbai, India, is used as the matrix material. Borosilicate GMBs (Trelleborg Offshore, USA) are used as fillers. Particle size analysis of the GMBs is presented in Fig. 1. Details of the measurement technique are given in Ref. [18]. The size distribution is monomodal, and less than 1% of particles are observed to be larger than 125 μm for all GMB types used in this work. Table 1 presents the properties of three different types of GMBs used in this work. These particles differ in density due to variation in wall thickness for nearly the same mean outer diameter (Table 1). The average diameters of GMBs are found to be 53, 50 and 45 μm, which are in a close range, eliminating particle size as a study parameter. The radius ratio for the GMBs is estimated by assuming uniform fully dense walls using [26].

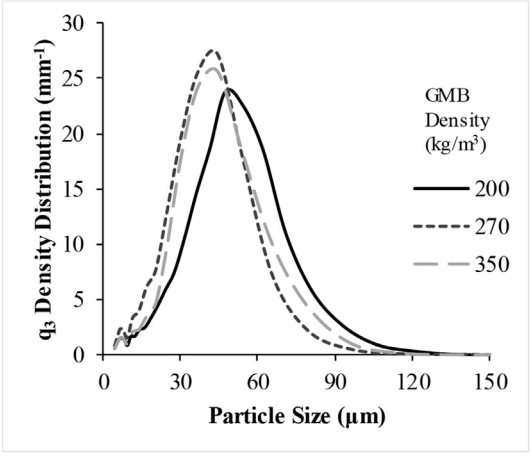

Fig. 1. Particle size analysis of GMBs used in the present study.

$$\eta = \left(1 - \frac{\rho_{TPD}}{\rho_g}\right)^{1/3} \quad (1)$$

where ρ_g is taken as 2540 kg/m^3 [27]. The wall thickness of the GMBs is estimated using [28].

$$w = r_0(1 - \eta) \quad (2)$$

where w varies between 0.716 and 1.080 μm for the GMBs utilized in the present work.

2.2. Sample preparation

A Brabender (Fig. 2a) is used for preparing GMB/HDPE blends. The mixture is then compression molded to form sheets. Specifications of the Brabender and compression molding machine are presented in Table 2. The cast specimens are named according to the convention HYYY-ZZ, where H denotes the HDPE matrix, YYY and ZZ are the true particle density in kg/m^3 and GMB vol%, respectively. Nine types of syntactic foams having three types of GMBs with filler loadings of 20, 40 and 60 vol% are fabricated.

During syntactic foam fabrication, HDPE is first plasticized at 160 °C [17] in the Brabender for 5 min. GMB are added to the melt in

Table 1
Properties of the GMBs used in the study.

GMB type	Average GMB diameter (μm)	True particle density (kg/m^3)	w (μm)	η
SID200	53	200	0.716	0.973
SID270	50	270	0.925	0.963
SID350	45	350	1.080	0.952

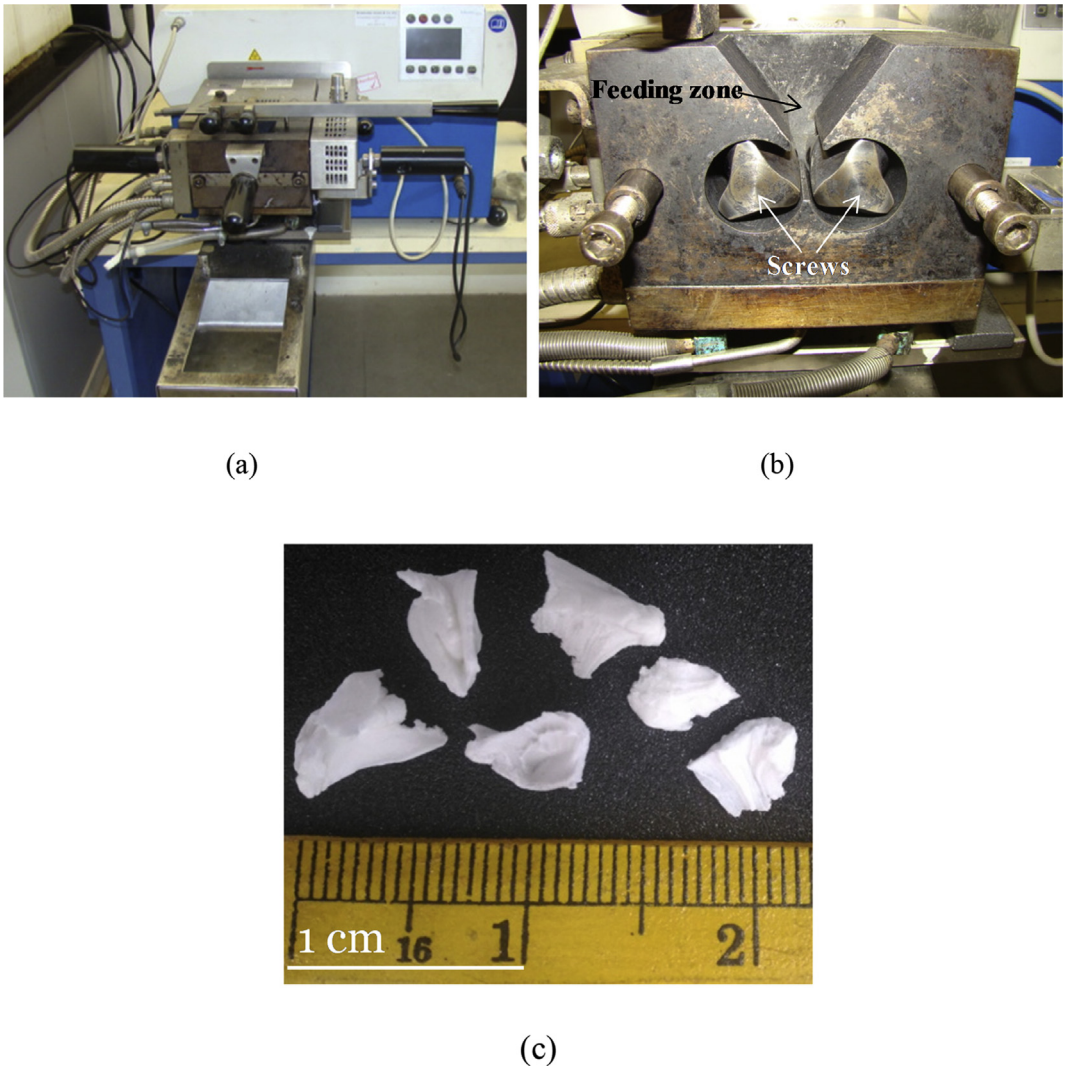

Fig. 2. (a) Brabender, (b) blending mechanism and (c) pellets of GMB/HDPE syntactic foam.

Table 2
Specifications of Brabender and compression molding machine.

	Brabender	Compression molding
Make	Western Company Keltron, Germany	Santec Automation Pvt. Ltd., India
Model	16 CME SPL	SP - 30
Product	Mixer 50 HT	SAIPL
Voltage (V)	240 + PE	415
Frequency	50/60	–
Power (kW)	3.88	3.7
Ampere (A)	16.2	–
Max. pressure (bar)	–	200

the mass ratio of 4:1 (HDPE:GMB) and mixed for two more minutes. This process is repeated until the entire quantity of GMBs is mixed thoroughly in HDPE. Mixing takes place in the confined chamber comprising of two screws (Fig. 2b). Screw rotation speed needs to be optimized to minimize the GMB breakage by high shear mixing. The published literature utilizing Brabender blending has not

reported screw speed optimization [23]. An optimization study is first conducted for the screw rotation speed, which is then fixed for fabricating all nine types of foams. Neat HDPE samples are also prepared under the similar processing conditions for comparison.

GMB/HDPE syntactic foam pellets from Brabender are shown in Fig. 2c. These pellets are hot pressed in a compression molding machine. The pressure-temperature cycle used in compression molding is presented in Fig. 3a. A polyethylene sheet is laid into the compression mold cavity initially for easier removal of the cast sheet. Weighed GMB/HDPE lumps (80 g) are loaded into the mold cavity of dimension of 165 × 165 × 3.2 mm^3 and are covered by another polyethylene sheet from above. At the start of the pressure-temperature cycle, pressure is set at 50 bar to disperse the GMB/HDPE lumps uniformly into the mold cavity and then the cycle is executed as presented in Fig. 3a [23]. Once the temperature reaches the peak value of 160 °C, pressure is re-applied to consolidate the blend in sheet form. This condition is held for 10 min, after which a 30-min cooling cycle is initiated. Finally, cast sheets of GMB/HDPE are removed from the mold. Fig. 3b shows a GMB/HDPE sheet, which is sectioned to produce specimens for the flexural and tensile tests.

2.3. Density measurement

Density of all fabricated specimens is measured according to ASTM D792-13. The densities of five specimens are measured and the average values with standard deviations are reported. The density of neat HDPE is measured to be 0.959 ± 0.002 g/cm^3, which is used in rule of mixtures to calculate theoretical density of syntactic foams.

2.4. Flexural and tensile testing

A computer controlled Zwick universal testing machine (Zwick Roell Z020, USA) having a load cell capacity of 20 kN is utilized for flexural and tensile testing. ASTM D790-10 standard is adopted for flexural testing in the three-point bend configuration using specimen dimensions of 127 × 12.7 × 3.2 mm^3. The crosshead displacement rate is maintained at 1.54 mm/min and a pre-load of 0.1 MPa is applied before the test. Specimens have a span length of 52 mm to maintain 16:1 span length/thickness ratio. Five specimens are tested and the average values of the measured properties are presented. Tests are terminated at 10% strain if the specimen does not fracture. The flexural modulus (E_f) is calculated using

$$E_f = \frac{L^3 m}{4bd^3} \tag{3}$$

The flexural stress (σ_{fM}) is estimated by

$$\sigma_{fM} = \frac{3PL}{2bd^2} \tag{4}$$

where P is the load at a given point on the load-deflection curve (N).

An Instron 4467 Universal Testing Machine with a 30 kN load cell is used to perform tensile tests on specimens of dimensions 127 × 12.7 × 3.2 mm^3. Tests are conducted at three different strain rates of 1.6 × 10^{-5} s^{-1}, 1.6 × 10^{-4} s^{-1} and 1.6 × 10^{-3} s^{-1} and the strain is captured using a clip-on Instron extensometer of gauge length 50.8 mm (2 inch). The load data is acquired by Bluehill 2.0 software which is then used to calculate stress values. Five specimens for each material type are tested and average values are reported.

2.5. Imaging

A JSM 6380LA, JEOL (Japan) scanning electron microscope is used for microstructure observations. All the specimens are sputter coated with gold using a JFC-1600 auto fine coater (JEOL, Japan).

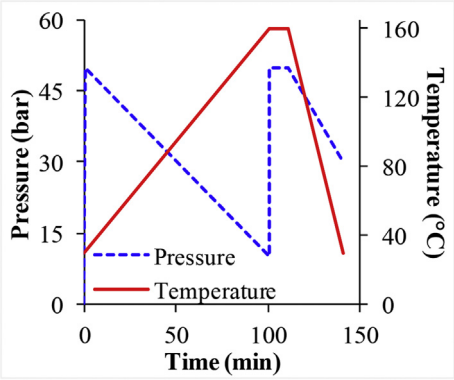

(a)

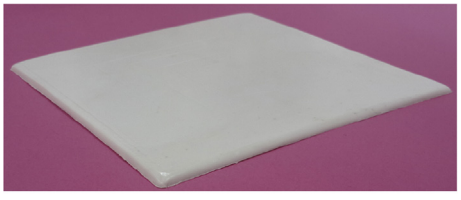

(b)

Fig. 3. (a) Pressure-temperature cycle utilized to prepare samples and (b) a molded GMB/HDPE sheet.

3. Results

3.1. Process development

A pilot study is conducted for finding the optimal screw speed in the Brabender to minimize GMB breakage. HDPE reinforced with 60 vol% of thin walled GMBs (H200-60) is chosen for this study as thin walled particles in high volume fraction results in increased fracture due to particle-particle interaction. It is expected that the conditions optimized for this composition would be useful for other less sensitive compositions. The Brabender screw speed is gradually decreased from 40 to 10 rpm as per the results obtained in Table 3. Density is a strong indication of foam quality because particle fracture leads to higher density than expected. It is observed that the density trend starts to saturate between 20 and 10 rpm. Therefore, 10 rpm is selected for processing syntactic foams. Slower speeds may further reduce the GMB breakage but such benefit is expected to be very small based on this trend and the processing time would increase drastically.

Further observations of specimen quality are presented in Fig. 4, where specimen micrographs processed at 10 and 40 rpm are

Table 3
Density of H200-60 syntactic foam used in pilot study of screw rotation optimization.

Syntactic foam type	Screw rotation speed (rpm)	Density (g/cm^3)
H200-60	40	0.713 ± 0.007
	30	0.651 ± 0.006
	20	0.625 ± 0.004
	10	0.608 ± 0.002

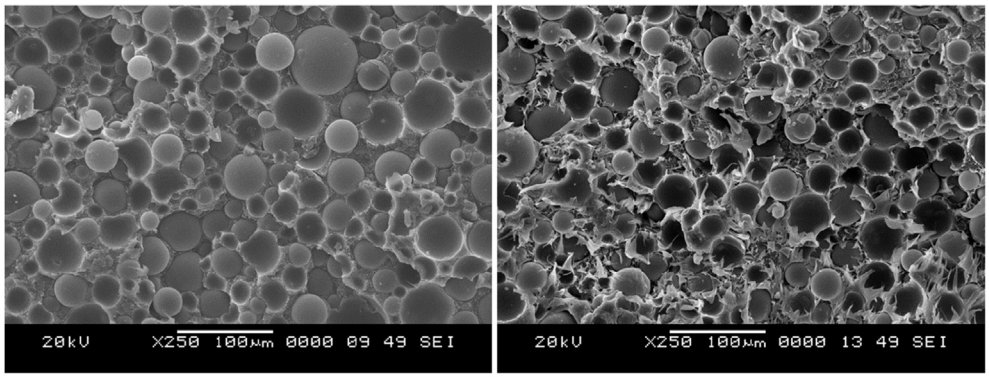

Fig. 4. Scanning electron micrograph of as molded freeze fractured H200-60 syntactic foam for (a) 10 and (b) 40 rpm screw rotation acquired at same magnifications. Higher GMB failure is seen in the syntactic foam developed at higher screw speed.

compared. Higher particle fracture is observed at 40 rpm screw speed in this figure, whereas most particles appear to be intact for the specimen processed at 10 rpm. Density based estimates show 42.6 vol%. GMB fracture at 40 rpm speed compared to only 17.8 vol% GMB fracture at 10 rpm. It is expected that GMBs with thicker walls would fracture less because of their higher strength.

A micrograph of a freeze fractured surface of molded H200-60 syntactic foam is presented in Fig. 5. Natural surface compatibility between GMB and HDPE is seen to be poor. Flexural and tensile properties strongly depend on the interfacial bonding characteristics to transfer load from the matrix to the particle. Though improvement in the GMB-HDPE interfacial bonding is desired for practical applications, such surface treatment of constituents can adversely affect the flow characteristics of HDPE around GMB, increasing localized stresses leading to greater particle fracture during syntactic foam fabrication [17]. Further, any inconsistency in surface treatment will affect both the flexural and tensile response, making the effect of wall thickness difficult to interpret in the present study [5,16].

Table 4 presents experimental and theoretical densities of developed syntactic foams. For all particles types, GMB failure is observed to be the highest for syntactic foams containing 60 vol% GMBs. Particle failure forms glass debris, which are embedded in the matrix. Although fractured particles do not provide the reduction in density as planned, they still help in replacing more expensive HDPE resin. Fig. 5 shows uniform distribution of GMBs affirming the good quality of GMB/HDPE syntactic foam sample processed through the adopted route.

3.2. Flexural behavior

A representative stress-strain curve for neat HDPE is presented in Fig. 6a. The test is stopped because the specimen did not fail before 10% strain. The flexural modulus of HDPE is measured to be 672 MPa. The measured properties of syntactic foams will be compared with the HDPE resin properties to observe the effect of presence of GMBs in syntactic foams.

Fig. 6b–d presents a set of representative stress-strain graphs of GMB/HDPE syntactic foams. The plastic strain of HDPE resin helps in obtaining plastic deformation in the syntactic foam specimens. As the particle volume fraction increases, the fracture strain is also observed to decrease. The mechanical properties calculated from these graphs are presented in Table 5. It is observed that for the syntactic foams containing the same type of particles, modulus increases, while strength and failure strength decrease as the GMB volume fraction is increased. Thicker walled GMBs exhibit higher modulus for all filler loadings (Table 5). Modulus for H200, H270 and H350 syntactic foams is observed to be 5–42%, 15–45% and 16–73% respectively higher than HDPE with varying filler content.

Specific modulus for H350-60 is observed to be 147% higher

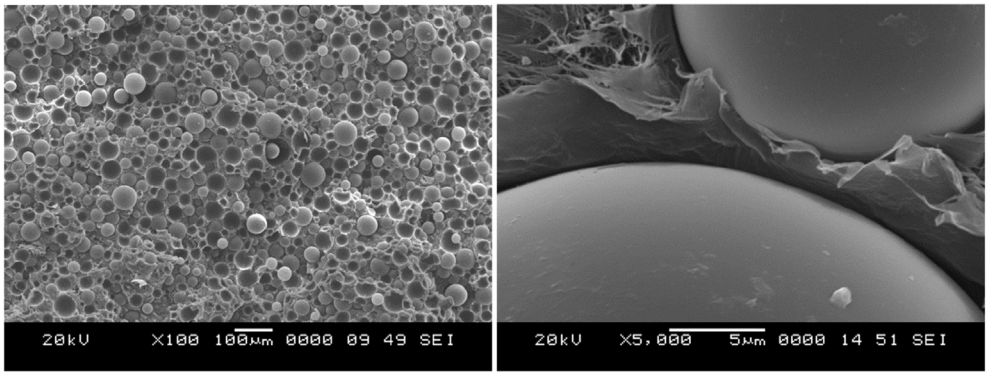

Fig. 5. Freeze fractured surface of as molded (a) H200-60 at lower magnification showing a large number of intact particles with uniform distribution in HDPE matrix and (b) higher magnification image showing poor interfacial adhesion between the constituents.

Table 4
Composition, nomenclature, density and GMB failure in fabricated syntactic foams.

GMB density (kg/m^3)	Φ (vol%)	Syntactic foam nomenclature	ρ_t (g/cm^3)	ρ_e (g/cm^3)	GMB failure (vol. %)
200	20	H200-20	0.800	0.847 ± 0.008	5.55
	40	H200-40	0.650	0.712 ± 0.014	8.71
	60	H200-60	0.500	0.608 ± 0.002	17.76
270	20	H270-20	0.814	0.845 ± 0.003	3.67
	40	H270-40	0.678	0.727 ± 0.001	6.74
	60	H270-60	0.542	0.642 ± 0.003	15.58
350	20	H350-20	0.830	0.853 ± 0.003	2.70
	40	H350-40	0.710	0.741 ± 0.004	4.18
	60	H350-60	0.590	0.672 ± 0.005	12.20

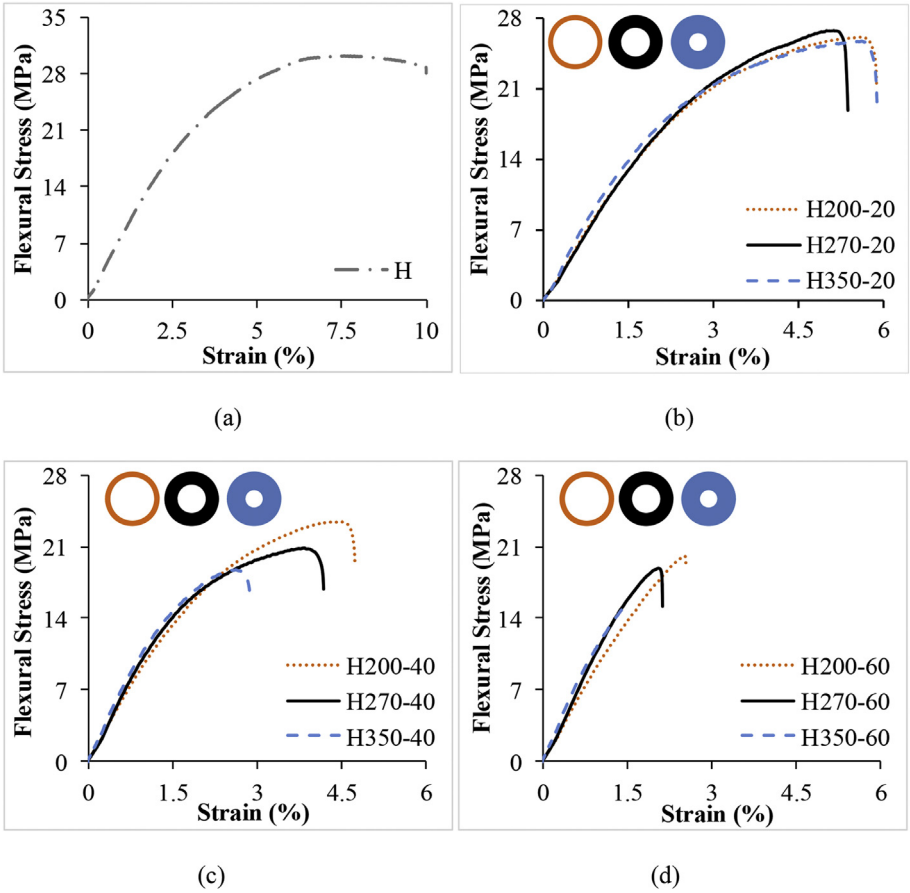

Fig. 6. Representative stress-strain curves of syntactic foams with varying wall thickness having (a) 20 (b) 40 and (c) 60 vol% GMBs. Note that (a) has different X and Y-scales than the other parts of the figure.

compared to neat HDPE (Fig. 7a), implying a weight and cost saving potential from these materials. Flexural strength is found to decrease with increasing GMB content and wall thickness. Specific strength (Fig. 7b) of syntactic foams containing H200 GMBs was higher than that of the neat resin. Other types of particles showed decreasing specific strength with increasing GMB content. It is likely that fracture of thin walled GMBs in H200 syntactic foams results in stress relaxation and delays failure. Volume fraction is more influential than wall thickness variation in affecting the flexural response of GMB/HDPE syntactic foams as per the experimental results. Effective load transfer between the constituents is a function of interfacial bonding which is observed to be poor between HDPE and GMBs (Fig. 5b). Due to the poor interfacial bonding, the matrix tends to flow around particles and provides large deformation. The four types of syntactic foams presented in Fig. 8 show no signs of particle crushing on the fracture surface during flexural failure.

3.3. Tensile behavior

The stress-strain behavior of HDPE resin at different strain rates is presented in Fig. 9. Modulus, yield strength and ultimate tensile strength extracted from the stress-strain graphs are presented in Table 6. HDPE specimens show failure strains of 9.3, 8.3 and 4.4% for strain rates of 1.6×10^{-5}, 1.6×10^{-4} and 1.6×10^{-3} s^{-1}, respectively. The syntactic foams have lower fracture strains for all GMB volume fractions and strain rates. Failure strain reduces with increasing filler content but no clear trend in fracture strain is observed with change in wall thickness. Ultimate tensile strength (UTS) for foams is lower than the neat resin and decreases with increasing filler

Table 5
Flexural properties of neat HDPE and their syntactic foams.

Foam type	E_f (MPa)	σ_{uf} (MPa)	ε_{uf} (%)	σ_{ff} (MPa)	ε_{ff} (%)
HDPE	672.12 ± 20.2	30.66 ± 0.70	7.62 ± 0.42	–	–
H200-20	707.51 ± 23.8	27.47 ± 0.36	5.87 ± 0.25	21.55 ± 0.41	5.97 ± 0.02
H200-40	798.49 ± 28.8	23.21 ± 0.59	4.17 ± 0.24	19.71 ± 0.59	4.72 ± 0.03
H200-60	951.32 ± 39.9	21.01 ± 0.67	2.51 ± 0.06	18.62 ± 0.71	2.53 ± 0.04
H270-20	769.77 ± 20.6	27.09 ± 0.42	5.34 ± 0.16	18.78 ± 0.51	5.35 ± 0.03
H270-40	864.93 ± 32.4	21.35 ± 0.46	3.04 ± 0.21	16.82 ± 0.63	4.28 ± 0.02
H270-60	972.51 ± 35.4	16.19 ± 0.61	2.39 ± 0.19	15.17 ± 0.55	2.09 ± 0.04
H350-20	781.32 ± 19.6	25.63 ± 0.43	5.17 ± 0.29	18.68 ± 0.98	5.87 ± 0.03
H350-40	1091.78 ± 20.9	19.42 ± 1.09	2.91 ± 0.11	15.82 ± 0.94	2.83 ± 0.03
H350-60	1165.73 ± 39.9	15.23 ± 1.15	1.28 ± 0.15	14.46 ± 0.78	1.27 ± 0.02

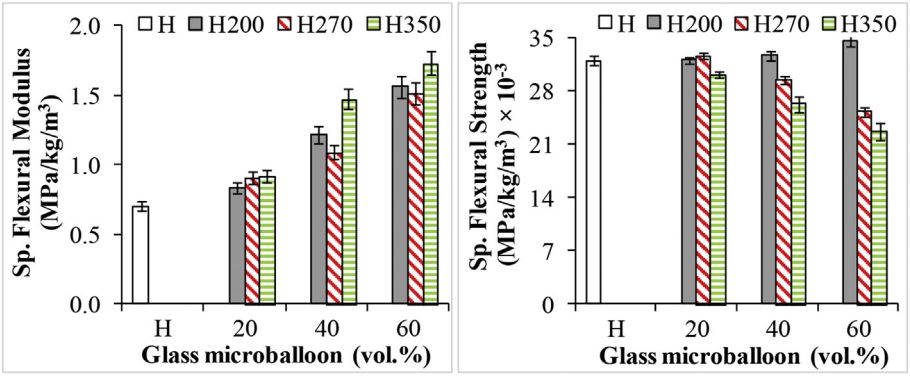

(a) (b)

Fig. 7. Experimentally measured specific flexural (a) modulus and (b) strength of HDPE and their syntactic foams.

content at all strain rates (Table 6). Higher filler content reduces the matrix content (effective load bearing constituent) resulting in lower tensile strength. Foams exhibit higher UTS with increasing strain rate for same wall thickness and volume fraction, which is attributed to the strain rate sensitivity of the matrix resin.

Effect of wall thickness on the modulus of syntactic foams with the same GMB volume fraction is greater at lower strain rates compared to higher ones (Table 6). For 1.6×10^{-5} s^{-1} strain rate, variation in modulus due to hollow particle wall thickness is 7, 22 and 28% for 20, 40 and 60% volume fractions, respectively. In contrast, it is found to be 29, 6 and 6% for 1.6×10^{-4} s^{-1} strain rate and 0, 8 and 12% for 1.6×10^{-3} s^{-1}. A general increasing trend is seen in the specific modulus of syntactic foams with GMB wall thickness at all strain rates. For higher strain rates, the variation in specific modulus with GMB wall thickness is not high enough to prescribe the use of any particular wall thickness for an application. Although there is no apparent trend in specific yield strength with wall thickness, syntactic foams showed better specific properties than the neat resin. The fracture strength of all the syntactic foams is up to 3.1, 2.6 and 3.4 times lower than that of the neat HDPE at strain rates 1.6×10^{-5}, 1.6×10^{-4} and 1.6×10^{-3} s^{-1}, respectively.

Failure patterns of neat HDPE and H200 specimens after tensile testing are presented in Fig. 10. H270 and H350 syntactic foams exhibited a similar failure pattern. Compression molded neat HDPE specimens fracture in brittle mode with no measurable necking. This behavior is different than that observed for injection molded neat HDPE samples [16,17]. Since HDPE is a partially crystalline polymer, the dual pressure-temperature cycle over a longer period of time (Fig. 3a) in compression molding compared to very short cycle time in injection molding likely affects the failure mode from ductile to brittle behavior by affecting the crystallinity.

Fracture surfaces of four types of syntactic foams are shown in Fig. 11. In all cases, no significant particle crushing is observed, only matrix deformation is visible. Higher plastic deformation is obtained in foams with thicker walled particles at higher filler contents (Fig. 11d).

4. Discussion

4.1. Theoretical modeling

A theoretical model proposed by Bardella and Genna (BG model) is used to estimate the elastic modulus of syntactic foams [12]. This model uses a homogenization scheme to estimate the bulk modulus and shear modulus of the composite. The modulus of the matrix material is taken from the experimental data and the Poisson's ratio is taken as 0.425 [16]. Modulus of 60 GPa and Poisson's ratio of 0.21 GMB are taken for GMB material [27]. The bulk modulus of syntactic foams is determined by

$$K = K_m \frac{\delta(1+\Phi\gamma)+\kappa(1-\Phi)\gamma}{\delta(1-\Phi)+\kappa(\gamma+\Phi)} \tag{5}$$

where $\gamma = \frac{4G_m}{3K_m}$, $\delta = \frac{4G_i}{3K_m}(1-\eta^3)$ and $\kappa = \frac{4G_i}{3K_i}+\eta^3$. Shear modulus is calculated using the equations in Ref. [12]. The elastic modulus of syntactic foams is determined as by

$$E_T = \frac{9KG}{3K+G} \tag{6}$$

Fig. 12 presents comparisons of experimental values of flexural modulus with BG model predictions. The model shows an

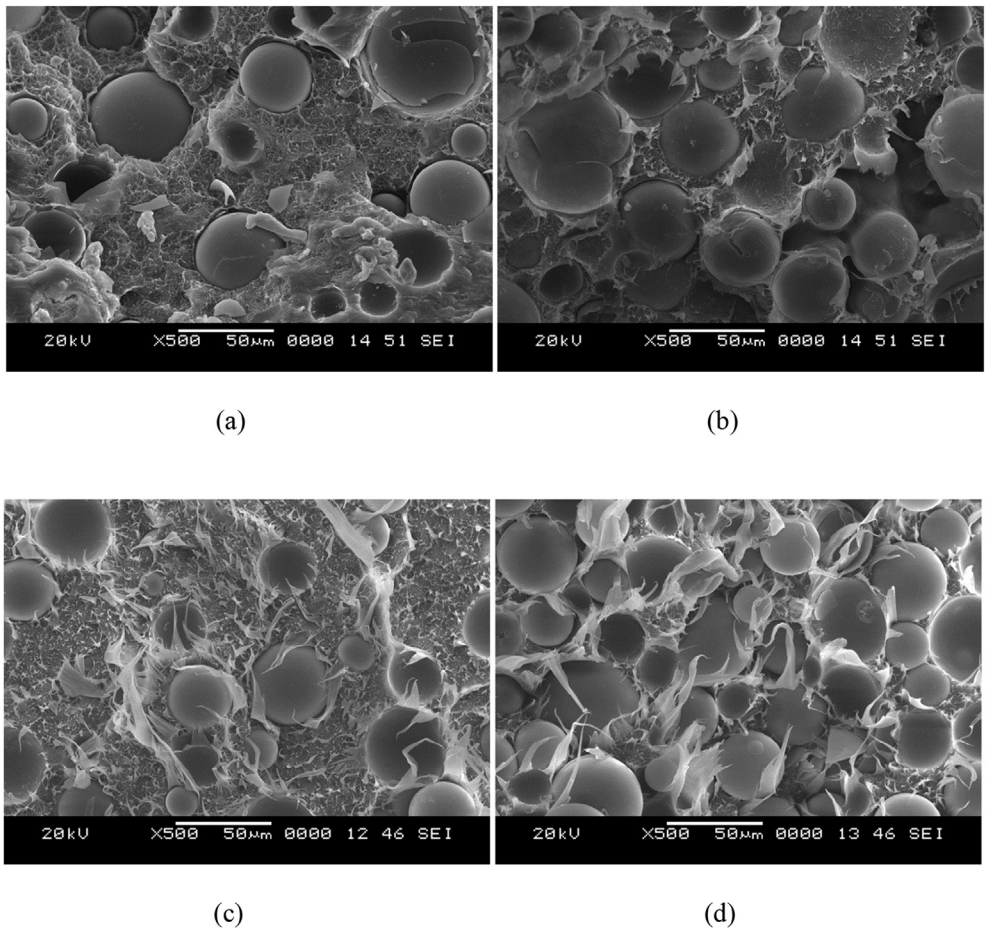

Fig. 8. Fracture features of (a) H200-20 (b) H200-60 (c) H350-20 and (d) H350-60 syntactic foams after flexure test. Particles are not broken or crushed on the fracture surface. Large deformation of matrix resin is evident in these micrographs.

increasing trend of modulus with increase in GMB content and decrease in radius ratio. BG model results are in the range of 2–17% for flexural modulus with the experimental values of all the syntactic foams. The predictions of tensile models are not compared with experimental data because the tests are conducted at multiple strain rate, while strain rate is not a parameter in the theoretical model.

4.2. Property map

Flexural and tensile properties are plotted with respect to density for HDPE composites containing different reinforcements in Fig. 13 [16,29–36] and Fig. 14 [16,29–31,37–41], respectively. Data are extracted from published literature and are plotted with respect to density in these figures to compare with the results obtained in the present study. It can be observed from the figures that composites with higher modulus also have higher density as a general trend for solid particle filled composites. However, the advantage of hollow particle filler is evident from this figure. H350-60 outperformed wood powder and cenosphere filled HDPE composites for flexural modulus. H200-20 exhibited superior flexural strength compared to wood powder, cenosphere, natural and hemp fiber HDPE composites with density reduction of almost 1.5 times for GMB/HDPE syntactic foams developed in the present study. H350-60 has much lower density with higher tensile modulus compared to wood, lignocellulose and calcium carbonate HDPE composites. Tensile strength for H350-20 is higher than cenosphere, β-tricalcium phosphate, scrap rubber powder; and comparable to lignocellulose with 1.18–1.3 times lower density. Choice of appropriate constituent materials and concentrations, the flexural and tensile properties can be tailored over a wide range as seen from Figs. 13 and 14. It is desired to have higher mechanical properties for lower densities, where syntactic foams can provide advantage as their specific strength and specific modulus would be comparable to several composites having higher absolute properties.

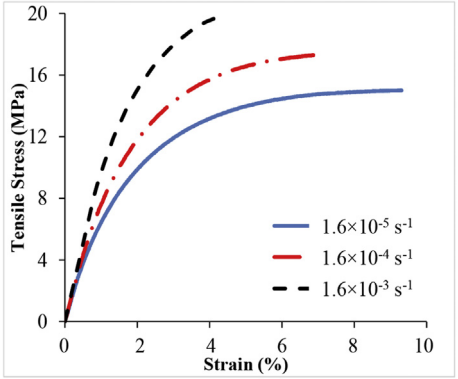

Fig. 9. Representative stress strain curves of neat HDPE for varying strain rates.

5. Conclusions

Compression molding is a widely used method for

Table 6
Tensile properties of neat HDPE and syntactic foams at varying strain rates.

Foam type	E_T(MPa)			σ_y(MPa)			σ_{uf}(MPa)		
	1.6×10^{-5} s^{-1}	1.6×10^{-5} s^{-1}	1.6×10^{-5} s^{-1}	1.6×10^{-4} s^{-1}	1.6×10^{-3} s^{-1}	1.6×10^{-5} s^{-1}	1.6×10^{-5} s^{-1}	1.6×10^{-4} s^{-1}	1.6×10^{-3} s^{-1}
H	762 ± 15	7.0 ± 0.4	7.0 ± 0.4	8.4 ± 0.2	12.4 ± 0.9	7.0 ± 0.4	15.0 ± 1.6	17.3 ± 1.6	19.9 ± 1.6
H200-20	825 ± 29	7.3 ± 0.7	7.3 ± 0.7	9.9 ± 0.3	10.8 ± 0.4	7.3 ± 0.7	10.9 ± 1.2	12.5 ± 1.1	12.0 ± 1.2
H200-40	726 ± 71	7.5 ± 0.3	7.5 ± 0.3	8.3 ± 0.7	11.0 ± 0.8	7.5 ± 0.3	9.3 ± 0.2	10.2 ± 0.5	11.6 ± 1.5
H200-60	678 ± 58	7.2 ± 1.2	7.2 ± 1.2	9.5 ± 0.1	9.2 ± 0.9	7.2 ± 1.2	7.4 ± 1.3	9.9 ± 0.2	9.4 ± 1.1
H270-20	784 ± 70	7.9 ± 0.6	7.9 ± 0.6	9.6 ± 0.2	11.6 ± 0.5	7.9 ± 0.6	10.3 ± 0.3	12.3 ± 0.3	13.8 ± 1.2
H270-40	824 ± 50	8.0 ± 0.5	8.0 ± 0.5	10.9 ± 0.7	12.9 ± 0.2	8.0 ± 0.5	9.0 ± 0.6	11.2 ± 0.6	12.9 ± 0.2
H270-60	968 ± 114	5.7 ± 0.7	5.7 ± 0.7	7.0 ± 0.4	6.0 ± 0.7	5.7 ± 0.7	4.9 ± 0.4	6.7 ± 0.6	5.8 ± 0.5
H350-20	923 ± 85	8.0 ± 0.6	8.0 ± 0.6	9.4 ± 0.7	12.7 ± 0.6	8.0 ± 0.6	9.9 ± 3.0	12.5 ± 0.4	13.5 ± 1.3
H350-40	1195 ± 59	7.4 ± 0.8	7.4 ± 0.8	7.7 ± 0.2	9.7 ± 0.8	7.4 ± 0.8	7.1 ± 0.1	7.9 ± 0.1	10.1 ± 0.5
H350-60	1369 ± 104	6.6 ± 1.1	6.6 ± 1.1	7.3 ± 0.7	9.3 ± 0.4	6.6 ± 1.1	7.3 ± 1.1	7.4 ± 0.6	9.3 ± 0.4

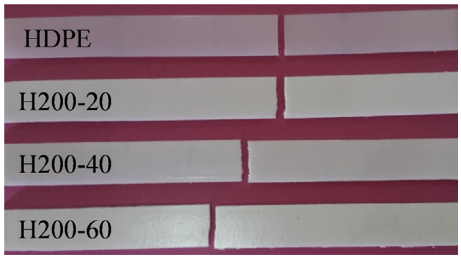

Fig. 10. Representative specimens of neat HDPE and syntactic foams after tensile test at 1.6×10^{-3} s^{-1} strain rate.

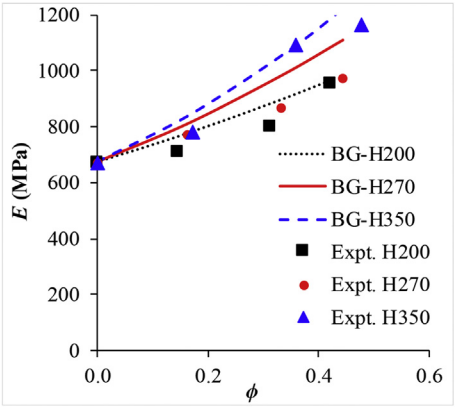

Fig. 12. Comparison of experimental values with theoretical models for flexural modulus.

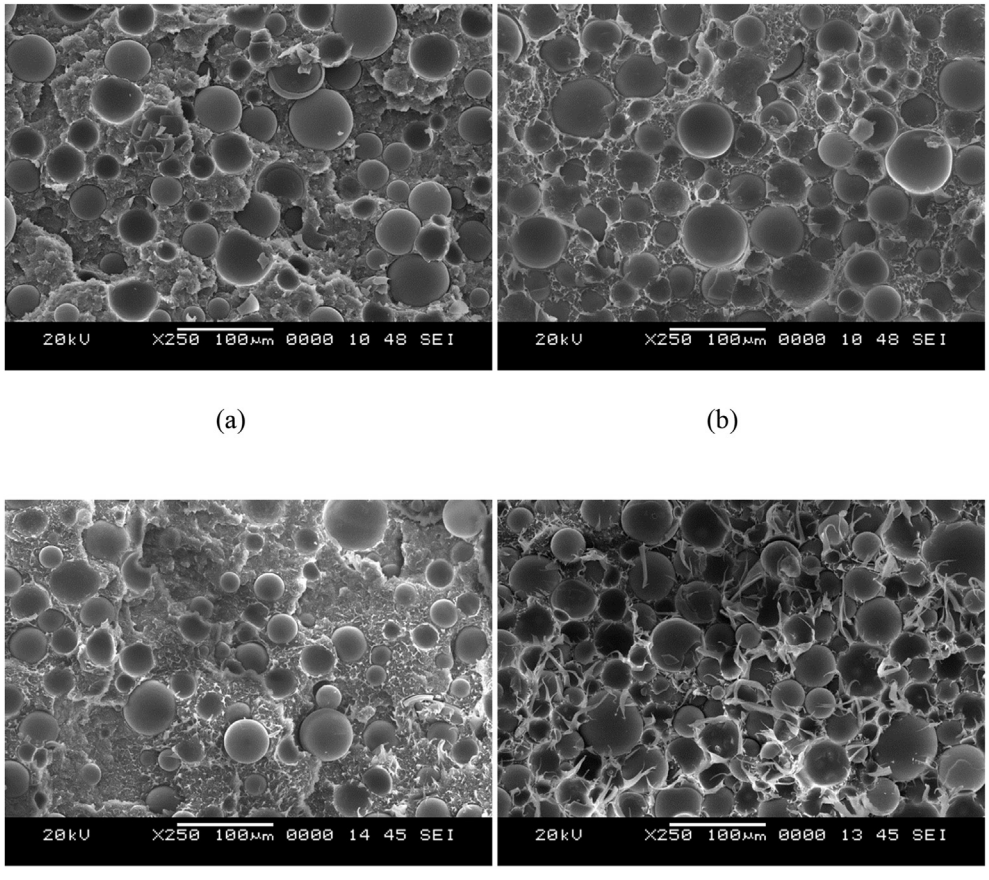

Fig. 11. Fracture features of (a) H200-20 (b) H200-60 (c) H350-20 and (d) H350-60 syntactic foams after tensile test 1.6×10^{-3} s^{-1} strain rate.

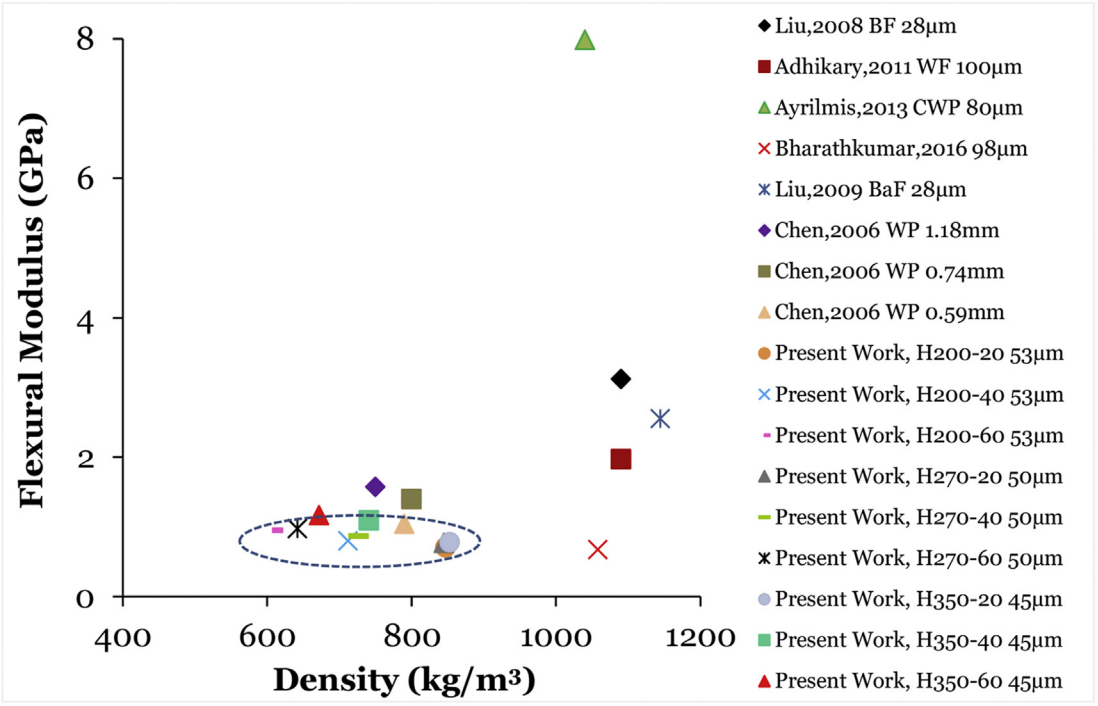

(a)

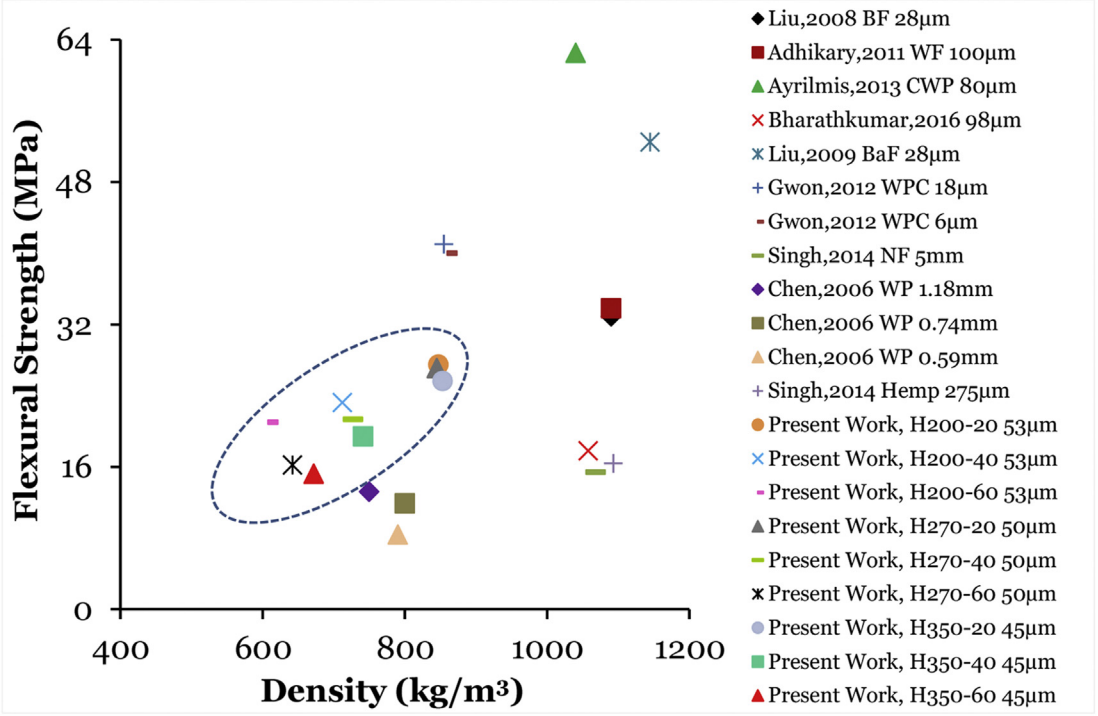

(b)

Fig. 13. (a) Flexural modulus and (b) strength of HDPE composites plotted against density from available studies [16,29–36].

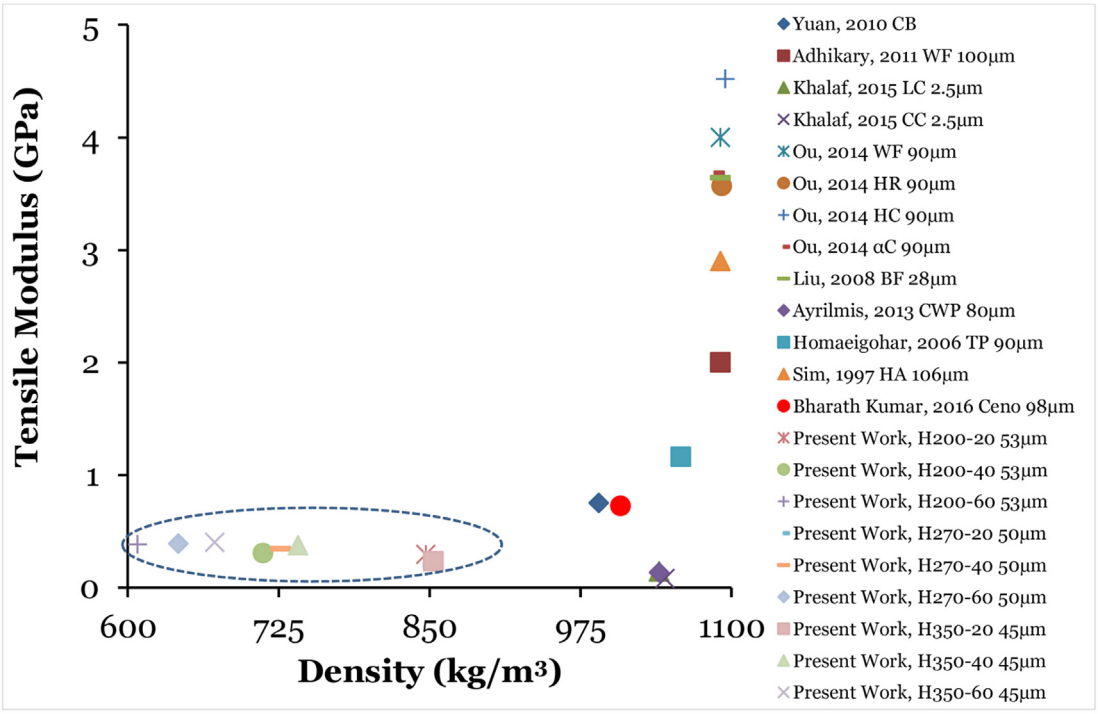

(a)

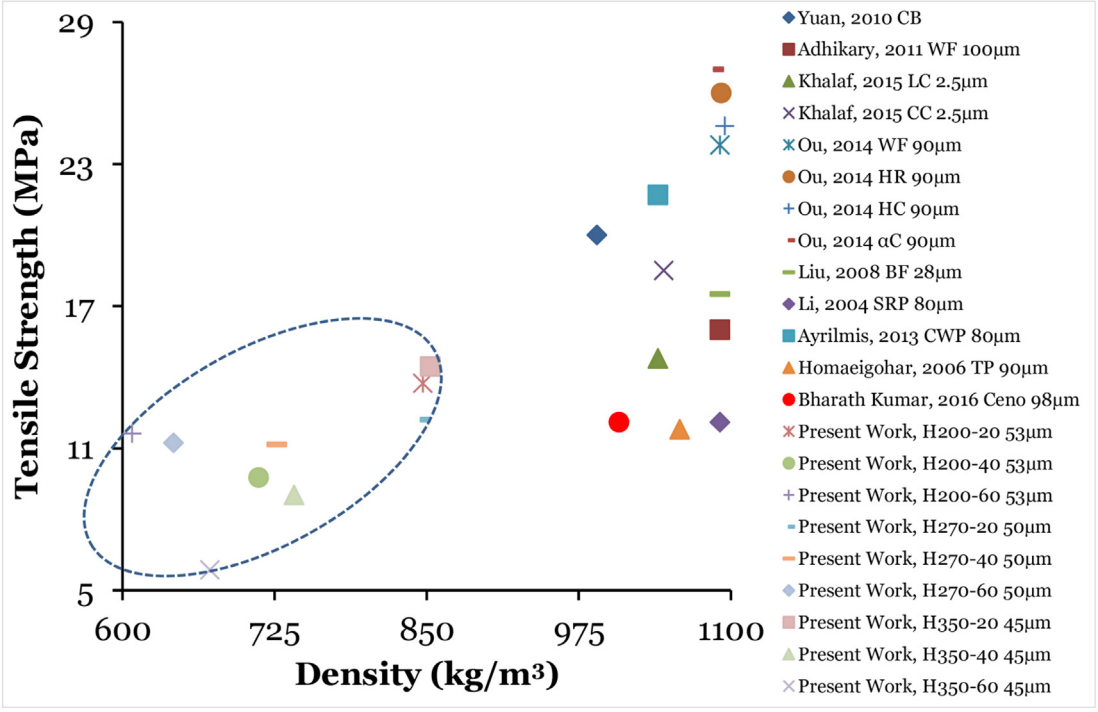

(b)

Fig. 14. (a) Tensile modulus and (b) strength of HDPE composites plotted against density [16,29–31,37–41].

manufacturing thermoplastic composites. However, this method has not been applied to fabricate thermoplastic syntactic foams because particle may fracture under compressive load during fabrication. Process optimization resulted in reduction in particle fracture in syntactic foams manufactured by this method. The fabricated syntactic foams are characterized for flexural and tensile response. The main conclusions can be summarized as:

- Measured density of all the syntactic foams is lower than neat HDPE resin signifying potential weight saving.
- Extensive plastic deformation of HDPE is observed from the micrographs at higher filler loadings in thicker walled particles. Flexural modulus and strength are found to increase and decrease respectively with increasing GMB content for syntactic foams. The highest modulus and strength are recorded for H350-60 and H200-20 respectively. Specific modulus and strength of H350-60 and H200-60 are observed to be 147 and 8% higher compared to neat HDPE samples. Flexural properties are sensitive to volume fraction variations as compared to wall thickness variation.
- Tensile modulus is found to be relatively insensitive to GMB wall thickness. UTS decreases with increasing filler content. Compared to neat HDPE, syntactic foams fracture at lower strain. The fracture strength of all the developed syntactic foams is 1.5–3 times lower than that of the neat HDPE. Highest specific modulus observed for H200-60 is 0.64 MPa/kg/m^3. No clear trend is observed for specific strength.

Acknowledgements

Authors acknowledge Dr. R. R. N. Sailaja for providing Brabender facility for preparing the blends. Department of Science and Technology grant DST/TSG/AMT/2015/394/G is acknowledged by Mrityunjay Doddamani. Author Nikhil Gupta acknowledges the Office of Naval Research grant N00014-10-1-0988 and National Science Foundation US-Egypt Cooperative Research Grant IIA-1445686. Authors thank the Dean of Engineering at NYU-Abu Dhabi to partially fund MRD's trip to NUYAD for collaborative work. The views expressed in this article are those of authors, not of funding agencies. The authors thank the ME Department at NIT-K and MAE Department at NYU for providing facilities and support.

References

[1] Gupta N, Zeltmann S, Shunmugasamy V, Pinisetty D. Applications of polymer matrix syntactic foams. JOM 2013:1–10.
[2] Lin W-H, Jen M-HR. Manufacturing and mechanical properties of glass bubbles/epoxy particulate composite. J Compos Mater 1998;32(15):1356–90.
[3] Gupta N, Pinisetty D, Shunmugasamy VC. Reinforced polymer matrix syntactic foams: effect of nano and micro-scale reinforcement. Springer International Publishing; 2013.
[4] Gupta N, Woldesenbet E, Mensah P. Compression properties of syntactic foams: effect of cenosphere radius ratio and specimen aspect ratio. Compos Part A Appl Sci Manuf 2004;35(1):103–11.
[5] Gupta N, Nagorny R. Tensile properties of glass microballoon-epoxy resin syntactic foams. J Appl Polym Sci 2006;102(2):1254–61.
[6] Porfiri M, Gupta N. Effect of volume fraction and wall thickness on the elastic properties of hollow particle filled composites. Compos Part B Eng 2009;40(2):166–73.
[7] Gupta N, Ye R, Porfiri M. Comparison of tensile and compressive characteristics of vinyl ester/glass microballoon syntactic foams. Compos Part B Eng 2010;41(3):236–45.
[8] Kishore, Shankar R, Sankaran S. Short beam three point bend tests in syntactic foams. Part I: microscopic characterization of the failure zones. J Appl Polym Sci 2005;98(2):673–9.
[9] Kishore, Shankar R, Sankaran S. Short-beam three-point bend tests in syntactic foams. Part II: effect of microballoons content on shear strength. J Appl Polym Sci 2005;98(2):680–6.
[10] Kishore, Shankar R, Sankaran S. Short-beam three-point bend test study in syntactic foam. Part III: effects of interface modification on strength and fractographic features. J Appl Polym Sci 2005;98(2):687–93.
[11] Huang JS, Gibson LJ. Elastic moduli of a composite of hollow spheres in a matrix. J Mech Phys Solids 1993;41(1):55–75.
[12] Bardella L, Genna F. On the elastic behavior of syntactic foams. Int J Solids Struct 2001;38(40–41):7235–60.
[13] Rizzi E, Papa E, Corigliano A. Mechanical behavior of a syntactic foam: experiments and modeling. Int J Solids Struct 2000;37(40):5773–94.
[14] Yalcin B. Chapter 7-hollow glass microspheres in polyurethanes. In: Amos SE, Yalcin B, editors. Hollow glass microspheres for plastics, elastomers, and adhesives compounds. Oxford: William Andrew Publishing; 2015. p. 175–200.
[15] Yalcin B, Amos SE. Chapter 3-hollow glass microspheres in thermoplastics. In: Amos SE, Yalcin B, editors. Hollow glass microspheres for plastics, elastomers, and adhesives compounds. Oxford: William Andrew Publishing; 2015. p. 35–105.
[16] Bharath Kumar BR, Doddamani M, Zeltmann SE, Gupta N, Ramesh MR, Ramakrishna S. Processing of cenosphere/HDPE syntactic foams using an industrial scale polymer injection molding machine. Mater Des 2016;92:414–23.
[17] Bharath Kumar BR, Doddamani M, Zeltmann SE, Gupta N, Uzma Gurupadu S, Sailaja RRN. Effect of surface treatment and blending method on flexural properties of injection molded cenosphere/HDPE syntactic foams. J Mater Sci 2016;51(8):3793–805.
[18] Bharath Kumar BR, Zeltmann SE, Doddamani M, Gupta N, Uzma Gurupadu S, Sailaja RRN. Effect of cenosphere surface treatment and blending method on the tensile properties of thermoplastic matrix syntactic foams. J Appl Polym Sci 2016;133(35). n/a-n/a.
[19] Bharath Kumar BR, Singh AK, Doddamani M, Luong DD, Gupta N. Quasi-static and high strain rate compressive response of injection-molded cenosphere/HDPE syntactic foam. JOM 2016;68(7):1861–71.
[20] Kumar BRB, Doddamani M, Zeltmann SE, Gupta N, Ramakrishna S. Data characterizing tensile behavior of cenosphere/HDPE syntactic foam. Data Brief 2016;6:933–41.
[21] Zeltmann SE, Bharath Kumar BR, Doddamani M, Gupta N. Prediction of strain rate sensitivity of high density polyethylene using integral transform of dynamic mechanical analysis data. Polymer 2016;101:1–6.
[22] Zeltmann SE, Prakash KA, Doddamani M, Gupta N. Prediction of modulus at various strain rates from dynamic mechanical analysis data for polymer matrix composites. Compos Part B Eng 2017;120:27–34.
[23] Deepthi MV, Sharma M, Sailaja RRN, Anantha P, Sampathkumaran P, Seetharamu S. Mechanical and thermal characteristics of high density polyethylene–fly ash cenospheres composites. Mater Des 2010;31(4):2051–60.
[24] Patankar SN, Das A, Kranov YA. Interface engineering via compatibilization in HDPE composite reinforced with sodium borosilicate hollow glass microspheres. Compos Part A 2009;40(6–7):897–903.
[25] Patankar SN, Kranov YA. Hollow glass microsphere HDPE composites for low energy sustainability. Mater Sci Eng A 2010;527(6):1361–6.
[26] Shunmugasamy V, Zeltmann S, Gupta N, Strbik III O. Compressive characterization of single porous SiC hollow particles. JOM 2014;66(6):892–7.
[27] Tagliavia G, Porfiri M, Gupta N. Analysis of flexural properties of hollow-particle filled composites. Compos Part B Eng 2010;41(1):86–93.
[28] Gupta N, Gupta SK, Mueller BJ. Analysis of a functionally graded particulate composite under flexural loading conditions. Mater Sci Eng A 2008;485(1–2):439–47.
[29] Liu H, Wu Q, Han G, Yao F, Kojima Y, Suzuki S. Compatibilizing and toughening bamboo flour-filled HDPE composites: mechanical properties and morphologies. Compos Part A Appl Sci Manuf 2008;39(12):1891–900.
[30] Adhikary KB, Park CB, Islam MR, Rizvi GM. Effects of lubricant content on extrusion processing and mechanical properties of wood flour-high-density polyethylene composites. J Thermoplast Compos Mater 2011;24(2):155–71.
[31] Ayrilmis N. Combined effects of boron and compatibilizer on dimensional stability and mechanical properties of wood/HDPE composites. Compos Part B Eng 2013;44(1):745–9.
[32] Liu H, Wu Q, Zhang Q. Preparation and properties of banana fiber-reinforced composites based on high density polyethylene (HDPE)/nylon-6 blends. Bioresour Technol 2009;100(23):6088–97.
[33] Chen HC, Chen TY, Hsu CH. Effects of wood particle size and mixing ratios of HDPE on the properties of the composites. Holz als Roh- Werkst 2006;64(3):172–7.
[34] Gwon JG, Lee SY, Kang H, Kim JH. Effects of sizes and contents of exothermic foaming agent on physical properties of injection foamed wood fiber/HDPE composites. Int J Precis Eng Manuf 2012;13(6):1003–7.
[35] Singh R, Aggarwal L, Sood M. Investigation of Flexural behavior of hybrid natural fiber composite with recycled polymer matrix. Am Int J Res Sci Technol Eng Math 2014;3(6):237–40.
[36] Singh S, Deepak D, Aggarwal L, Gupta VK. Tensile and flexural behavior of hemp fiber reinforced virgin-recycled HDPE matrix composites. Procedia Mater Sci 2014;6:1696–702.
[37] Yuan Qiang, Bateman SA, Wu Dongyang. Mechanical and conductive properties of carbon black-filled high-density polyethylene, low-density polyethylene, and linear low-density polyethylene. J Thermoplast Compos Mater 2010;23(4):459–71.
[38] Khalaf MN. Mechanical properties of filled high density polyethylene. J Saudi Chem Soc 2015;19(1):88–91.
[39] Ou R, Xie Y, Wolcott MP, Sui S, Wang Q. Morphology, mechanical properties, and dimensional stability of wood particle/high density polyethylene composites: effect of removal of wood cell wall composition. Mater Des 2014;58:

339–45.
[40] Homaeigohar SS, Sadi AY, Javadpour J, Khavandi A. The effect of reinforcement volume fraction and particle size on the mechanical properties of β-tricalcium phosphate–high density polyethylene composites. J Eur Ceram Soc 2006;26(3):273–8.
[41] Sim CP, Cheang P, Liang MH, Khor KA. Injection moulding of hydroxyapatite composites. J Mater Process Technol 1997;69(1):75–8.